

# Connection between Gamma-Ray Variations and Disturbances in the Jets of Blazars

BOSTON UNIVERSITY

S. Jorstad<sup>1,2</sup>, A. Marscher<sup>1</sup>, F. D'Arcangelo<sup>1,3</sup>, and B. Harrison<sup>1</sup>

<sup>1</sup>Boston Univ.; <sup>2</sup>St. Petersburg State Univ., Russian Federation; <sup>3</sup>Lincoln Laboratory, MIT

**Abstract:** We perform monthly total and polarized intensity imaging of a sample of  $\gamma$ -ray blazars (33 sources) with the Very Long Baseline Array (VLBA) at 43 GHz with the high resolution of 0.1 milliarcsecond. From Summer 2008 to October 2009 several of these blazars triggered Astronomical Telegrams due to a high  $\gamma$ -ray state detected by the Fermi Large Area Telescope (LAT): AO 0235+164, 3C 273, 3C 279, PKS 1510-089, and 3C 454.3. We have found that 1)  $\gamma$ -ray flares in these blazars occur during an increase of the flux in the 43 GHz VLBI core; 2) strong  $\gamma$ -ray activity, consisting of several flares of various amplitudes and durations (weeks to months), is simultaneous with the propagation of a superluminal knot in the inner jet, as found previously for BL Lac (Marscher et al. 2008); 3) ejection of a superluminal knot from the 43 GHz core precedes the most intense  $\gamma$ -ray flare by  $39 \pm 24$  days. We observe similar behavior in the quasar 3C 345, for which our analysis of the Fermi data yields detection at 2-3 $\sigma$  on a weekly basis, although the source was not detected by EGRET or over the first three months of Fermi LAT operation (Abdo et al 2009). The prominent EGRET quasar 0528+134 has been  $\gamma$ -ray weak, in accordance with the recent quiescent state of the jet. Our results strongly support the idea that the most dramatic  $\gamma$ -ray outbursts of blazars originate in the vicinity of the mm-wave core of the relativistic jet.

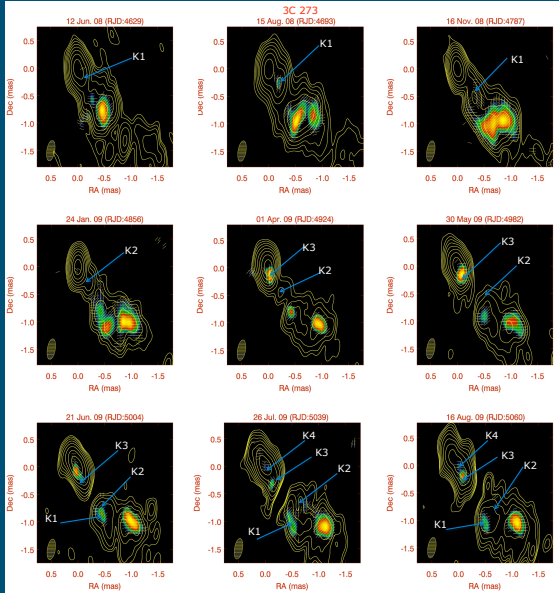


Fig. 1. Total (contours) and polarized (color scale) intensity images of the quasar 3C 273; yellow line segments show direction of the polarization; the size of the beam is  $0.38 \times 0.14$  mas<sup>2</sup> at PA= $-10^\circ$ ,  $S_{peak} = 7.9$  Jy/beam,  $S_{pol} = 135$  mJy/beam, contours are 0.25, 0.5, ...64 % of the total intensity peak.

**Data reduction:** We processed the VLBA data and created images in a manner identical to that described in Jorstad et al. (2005). We modelled the images in terms of a small number of components with circular Gaussian brightness distributions. The core is a stationary feature located at one of the end of the jet. Identification of components across the epochs is based on analysis of their flux, position angle, distance from the core, polarization, and size. Figures 1-5 show the total and polarized intensity images of 3C 273, 3C 279, 3C 345, 1510-089, and 0235+164 along with identification of moving knots. The speed and time of ejection of each knot were calculated from a ballistic part of its trajectory, with  $H_0 = 71$  km s<sup>-1</sup> Mpc<sup>-1</sup> and the concordance cosmology (Spergel et al. 2007). Figs. 6(a-d), 7, & 8 show the light curves of the core (red) and separation vs. time of moving knots with respect to the core. We use  $\gamma$ -ray flux measurements posted on the LAT website for 3C 273, 3C 279, 3C 454.3, 1510-089, 0235+164, and 0528+164 with a bin size of one week. We have calculated the  $\gamma$ -ray light curve for 3C 345 using the LAT data and the threads provided on the Fermi website.

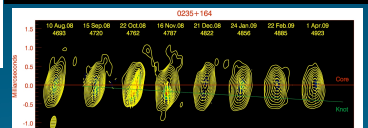
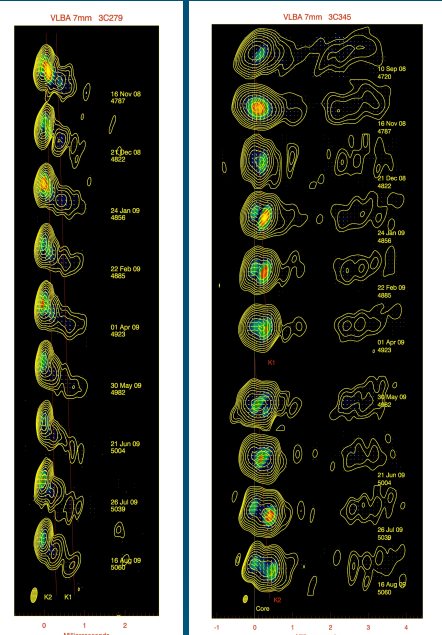


Fig. 4. Total (contours) and polarized (color scale) intensity images of 0235+164; yellow line segments show direction of polarization; the size of the beam is  $0.36 \times 0.15$  mas<sup>2</sup> at PA= $-10^\circ$ ,  $S_{peak} = 4.0$  Jy/beam,  $S_{pol} = 143$  mJy/beam, contours are 0.25, 0.5, ...64% of the total intensity peak.



Figs. 2 & 3. Total (contours) and polarized (color scale) intensity images of the quasars 3C 279 & 3C 345; yellow line segments show direction of the polarization; 3C 279: beam =  $0.36 \times 0.15$  mas<sup>2</sup> at PA= $-10^\circ$ ,  $S_{peak} = 12.0$  Jy/beam,  $S_{pol} = 200$  mJy/beam; 3C 345: beam =  $0.25 \times 0.14$  at PA= $-10^\circ$ ,  $S_{peak} = 3.3$  Jy/beam,  $S_{pol} = 68$  mJy/beam; contours are 0.25, 0.5, ...64 % of the total intensity peak.

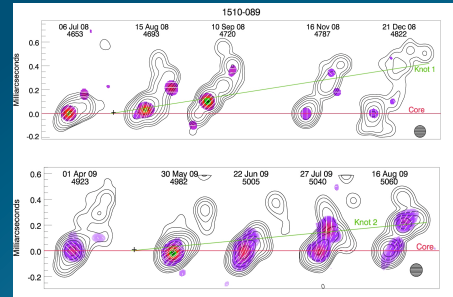


Fig. 5. Total (contours) and polarized (color scale) intensity images of 1510-089; white line segments show direction of polarization;  $\text{beam} = 0.1 \times 0.1$  mas<sup>2</sup>; top:  $S_{peak} = 1.4$  Jy/beam,  $S_{pol} = 71$  mJy/beam; bottom:  $S_{peak} = 3.1$  Jy/beam,  $S_{pol} = 120$  mJy/beam, contours are 1, 2, ...64% of the total intensity peak.

**Discussion:** 1) We find that a high state of  $\gamma$ -ray emission in blazars correlates with brightening of the VLBI core at 43 GHz caused by a disturbance propagating through the core. The disturbance is seen in VLBA images as a knot of enhanced total and polarized intensity (Figs. 1-5). Table 1 gives the timing between  $\gamma$ -ray peaks and ejections of superluminal components from the core.

Source	$\gamma$ Knot	VLBI Knot	$\Delta T$ (days)	$\Delta \theta$ (mas)	Speed of Superluminal Knot (c)
0235+164	0191	K1	480(20)	0.78(1)	0.5(1)
3C 273	0136	K2	470(10)	0.74(1)	0.8(1)
3C 279	0136	K2	490(20)	0.82(1)	0.6(1)
3C 279	0136	K2	500(1)	0.7(1)	0.7(1)
1510-089	0191	K2	470(20)	0.88(1)	0.7(1)
3C 345	0191	K1	477(21)	0.77(1)	0.6(1)
3C 345	0191	K2	495(20)	0.81(1)	0.6(1)

Note. — Column 1: source name; 2: knot(s); 3: knot designation; 4: time of the ejection of superluminal knot from the core at 43 GHz; 5: time of the peak of the  $\gamma$ -ray flare; 6:  $\Delta T = \Delta \theta / \beta$ ; 7:  $\beta$ —apparent speed of the superluminal knot;  $\Delta \theta_{app}$ —the distance from the peak of the  $\gamma$ -ray flare.

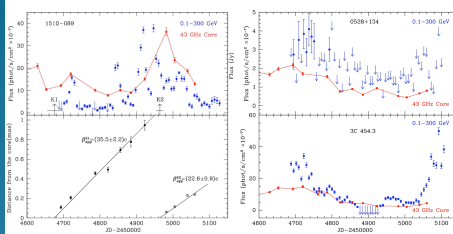


Fig. 7. The same as in Fig. 6 for the quasar 1510-089.

Fig. 8.  $\gamma$ -ray (blue) and 43 GHz VLBI core (red) light curves of 0528+134 (top) and 3C 454.3 (bottom).

References: Abdo et al. 2009, ApJS, 183, 46; 2009b, ApJ, 699, 817; Bonning et al. 2009, ApJL, 697, 81; Jorstad et al. 2001, ApJ, 556, 738; 2005, AJ, 130, 1418; Lähteenmäki & Valtaoja 2003, ApJ, 580, 85; Marscher et al. 2008, Nature, 452, 966; Spergel et al. 2007, ApJS, 170, 377.

This research was funded in part by NASA through Fermi Guest Investigator grants NNX08AV65G and NNX08AV61G, Astrophysical Data Analysis Program grant NNX08AJ64C, and by the National Science Foundation through grant AST-0907893.

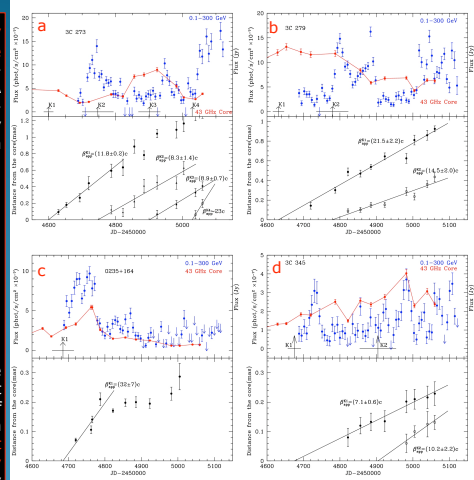


Fig. 6. Top plot of each panel:  $\gamma$ -ray (blue) and 43 GHz VLBI core (red) light curves of 3C 273(a), 3C 279(b), 0235+164(c), and 3C 345(d); arrows indicate the time of ejection of superluminal knots from the core; the time of the ejections is determined from a linear fit to the motion of knots near the core, as shown at the bottom plot of each panel.

3) Abdo et al. (2009b) reported a steepening of the  $\gamma$ -ray spectral slope of 3C 454.3 above 2 GeV from  $-1.3$  to  $-2.5$ . The break can be explained by steepening of the electron energy distribution above an energy  $\gamma \sim 10^4$  ( $\gamma$  is the electron Lorentz factor). If  $\beta \leq 1$  the seed photons should have observed frequencies  $\sim 10^{12} (\Gamma/15)^{-2} (\delta/15)^{-2}$  Hz, where  $\Gamma$  &  $\delta$  are the Lorentz and Doppler factors of the jet. In the case of the EC process, this favors either the putative dust torus or a slower sheath of the jet as the source of the seed photons.